ELSEVIER

Polymer 43 (2002) 4657–4665

polymer

www.elsevier.com/locate/polymer

# Structure of polymers in the vicinity of convex impenetrable surfaces: the athermal case

M.S. Ozmusul, R.C. Picu*

*Department of Mechanical, Aeronautical and Nuclear Engineering, Rensselaer Polytechnic Institute, Troy, NY 12180, USA*

Received 15 November 2001; received in revised form 2 May 2002; accepted 8 May 2002

**Abstract**

The influence of the presence of a curved (convex) solid wall on the conformations of long, flexible polymer chains is studied in a dense polymer system and in the athermal limit by means of lattice Monte Carlo simulations. It is found that the chain conformation entropy drives a reduction of the density at the wall, similar to the flat wall case. The chain end density is higher next to the interface compared to the bulk polymer (segregation), with the difference increasing with chain length. The wall curvature does not significantly affect the segregation. The bonds are preferentially oriented in the direction tangential to the wall. The distance from the interface over which this effect is observed is about two bond lengths. Similar results are obtained when probing the preferential orientation of chain segments. In this case, the perturbed region has a thickness on the order of the considered probing chain segment length. This suggests that experimental results on the thickness of the 'bonded layer' next to a wall depend on the wavelength of the radiation employed for probing. The chains are ellipsoidal in the bulk and rotate close to the surface with the large semi-axis of the ellipsoid normal to the line connecting their center of mass with the filler center. Since there is no energetic interaction with the filler, no adsorption transition is observed, but the chains tend to wrap around the filler once the gyration radius becomes comparable to the filler radius. 

*Keywords:* Polymer nanocomposites; Polymer interfaces; Lattice Monte Carlo

## 1. Introduction

The structure of the interface between a bulk solid polymer and another medium is a subject of considerable interest. The macroscopic properties of a polymer matrix composite are determined to a large extent by the properties of the interface between the matrix and filler particles or fibers. Flow and capillarity in narrow channels or filters and the interaction with membranes are dominated by the interaction of the fluid with the walls. The structure of the interface with the substrate and that of the free surface of a polymeric thin film are important in applications that require coating. This wide range of applications has driven a constant interest in the properties of polymeric interfaces.

It is well known that the conformations of polymer chains are restricted in the neighborhood of impenetrable interfaces. The structure of the polymer is determined by the energetics of the interaction with the wall, by the cohesive energy in the bulk polymer, and by the loss of configurational entropy when the chain approaches the interface. The entropic force due to the reduction in the number of accessible chain configurations drives the chain away from the interface. The excluded volume effect in the bulk polymer, and an attractive interaction with the wall promote the opposite trend. The interplay of these factors determines a structure that is significantly different from that of the bulk polymer.

These issues have been studied extensively experimentally [1–3], as well as analytically [4–8] and by means of simulations [9–14]. In the immediate vicinity of a flat impenetrable wall, the polymer chains are preferentially aligned in the direction parallel to the interface and have reduced mobility. This leads to changes in the glass transition temperature and to a broader relaxation spectrum. The degree of alignment depends on the details of the energetic interaction with the wall. A chain may adopt a 'docking' type configuration at high temperatures and weak attractive interactions, and may completely adsorb if the attraction is strong [15]. The chain collapse in the interface leads to pronounced alignment on the bond and larger scales. The volume of polymer affected by the presence of

* Corresponding author. Tel.: +1-518-276-2195; fax: +1-518-276-6025.
*E-mail address:* picuc@rpi.edu (R.C. Picu).

0032-3861/01/$ - see front matter 
PII: S0032-3861(02)00316-6

the interface (or the thickness of the 'bonded layer') is generally estimated to about two bulk root mean square gyration radii.

An entropic driving force exists for the segregation of chain ends in the interface [6]. This effect may be overridden by energetic interactions with the wall, no segregation being seen, for instance, in presence of a strong attraction to the wall. The total bead density may differ next to a solid wall compared to the bulk [16–18]. The density profile depends on the relative importance of the energetic interactions between the wall and the polymer, and within the polymer itself. Their interplay leads to a denser or a depleted layer. The variation in density has a significant effect on chain mobility as well as on diffusion of small molecules. Similar effects of the local density on chain mobility are observed at the free surface of a polymer thin film [18].

While the flat wall problem has been studied extensively, not much work has been done on the effect of the impenetrable wall *curvature* on the structure of the polymer next to the interface [19]. The present study addresses this problem in the athermal limit in which only excluded volume interactions are considered. The goal is to first understand how the purely entropic effect controls the structure of the interface. The contribution of the energetic interactions will be discussed in the sequel to this paper.

This work is part of an effort to understand the structural origins of the exceptional mechanical properties exhibited by polymer-based nanocomposites with ceramic nanofillers [20,21]. These materials show significantly enhanced stiffness and strength compared to the similar material filled with regular micron size ceramic particles. Most importantly, a gain in these properties does not compromise ductility, as is typically the case with conventional materials.

A number of theories have been proposed to explain this behavior. One of these, the 'bonded polymer layer' theory [22], is based on the observation that, at the same volume fraction, the total interfacial area in the nanocomposite is much larger than that in the polymer filled with micron sized particles. On the basis of the insight gained from studies of the polymer structure next to a flat impenetrable interface, it is hence conjectured that the total volume of 'bonded polymer' (confined polymer chains next to the wall) represents a large fraction of the volume of the nanocomposite and therefore, the properties of this confined material determine the macroscopic properties of the system. However, the available experimental results on the existence of the bonded polymer layer are contradictory [23,24]. It is also unclear how thick the layer surrounding each particle is and, most importantly, what are the properties of the polymer in the interfacial region.

More recently, the 'double network' theory was proposed. This idea is based on the observation that the reduction in particle size entails a similar reduction in the inter-particle spacing, and that special macroscopic properties are obtained when the average distance between particles becomes comparable with the bulk radius of gyration of the polymer chains. This creates conditions for a chain to connect two or more particles, hence forming a network that provides additional strength [25].

In an effort to distinguish between these theories, the present work provides new information on the effect of the particle curvature on the structure of the polymer at the interface. The article is organized as follows: the modeling and simulation procedure are presented in Section 2, the results are discussed in Section 3, and the conclusions are presented in Section 4.

## 2. Modeling and simulation procedure

This study is performed by means of lattice Monte Carlo (MC) simulations using the bead-spring model. The simulation cell is shown in Fig. 1. The volume surrounding a spherical particle of radius $R$ is filled with a monodisperse population of polymer chains of length $N-1$ bonds ($N$ beads). The volume of the particle is a forbidden zone for the chains. The polymers occupy a bcc lattice that fills the allowed volume. A unit cell of that lattice is shown schematically in the lower left corner of the simulation cell in Fig. 1. The coordination on the bcc lattice is 14, the bonds linking either corner sites or a corner with the body center site. This type of lattice was chosen because it minimizes bond length fluctuations, while allowing for denser systems compared to the simple cubic lattice (which preserves the bond length). Periodic boundary conditions are imposed on all faces of the simulation cell. Hence, the simulated system represents a 3D square array of spherical particles immersed in the polymer matrix. The dimension $L$

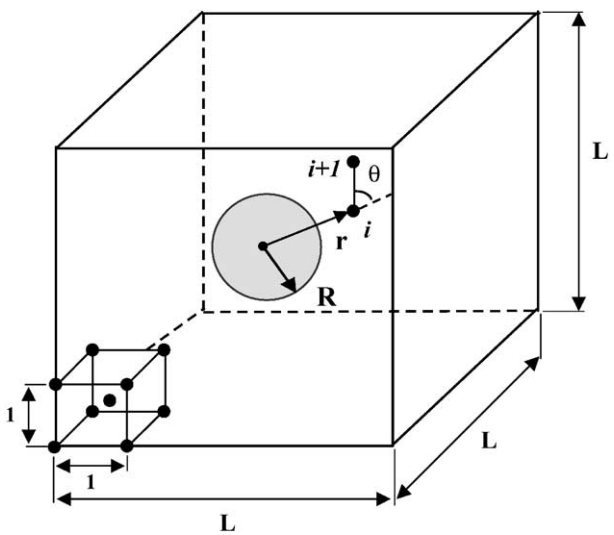


Fig. 1. Schematic representation of the model and the coordinate system. The volume between the spherical particle and the boundary of the simulation cell is occupied by a bcc lattice (unit cell shown) on which the chains evolve.

of the cell was selected large enough for dilute limit conditions (in what regards the filler particles) to prevail. In all calculations reported here, $L$ was taken to be 50 bcc unit cells, while the parameter $R$ varied between 2 and 12. This insures that the layer of perturbed polymer is thinner than the distance between the particle surface and the simulation cell boundaries, which in turn, eliminates image effects. The full filler size effect, including the interaction of the perturbed layers surrounding neighboring fillers and in presence of energetic interactions will be discussed in the sequel to this article.

The simulation cell is filled with chains of the desired length and at the desired bead number density, $\rho$, by performing self avoiding random walks (SAW) on the bcc lattice. The excluded volume restriction is imposed during the generation process. According to it, in the usual SAW, one generates the walk until the whole chain is generated or the excluded volume condition cannot be fulfilled. In this second case, one has to discard the current chain and start a completely new one. This procedure may be used successfully in low-density systems. At high densities however, the method becomes impractical. Here, a slightly modified method which is somewhat related to earlier ideas by McCrackin [26], is used. According to this procedure, the chain generation is not stopped at the first violation of the excluded volume condition, but rather continued until the whole chain is constructed. The probability for overlap generation is controlled using an idea similar to that of the importance sampling MC. A 'tolerance to overlaps' parameter is included in the algorithm and, if an overlap is necessary, the step is accepted/rejected based on the overall number of overlaps in the system and the occupancy index for the current site. The value of this parameter is adjusted such to minimize the total number of overlaps in the system, while allowing for the generation of the whole chain population.

The overlaps produced during chain generation are eliminated in a subsequent equilibration. During this stage, the system is evolved by a simple sampling MC procedure. Two types of moves are made: the 'slithering snake' or reptation, and the 'crack shaft' move [27]. The reptation move consists in sliding the chain along its contour by one bond length, while the crack shaft move entails a local rotation of a group of 3 bonds about an axis defined by the neighboring chain segments. The two types of moves are performed with equal probability. A virtual energetic cost is imposed for each overlap, such that the procedure leads to their quick elimination. This energetic threshold is chosen large enough such that no further overlaps are produced during equilibration. No other energetic interactions are imposed, the chains being free to move on the lattice in the limit of the excluded volume constraint (no two beads can occupy a lattice site). The simulation evolves at constant number of beads and at constant volume. The average bond and segment orientation is monitored during equilibration to insure randomness. Both measures reach a stationary value after several tens of thousands of MC equilibration steps. The equilibration phase was run for 3 million MC steps (MCS), which is considered sufficient for the center of mass of a representative chain to translate over more than one root mean square radius of gyration. In this study, the chain diffusion was not monitored during the equilibration phase however, one million MCS is observed to correspond to the disentanglement time of chains of 100 beads in similar MC simulations reported in Ref. [28].

Once the excluded volume condition is imposed, a production phase begins. The same algorithm is employed for production. The polymer structure is obtained by averaging over time and over a number of replicas of the system in order to reduce statistical noise.

The results reported here are obtained from runs with 225,000 beads and chains of $N-1=32$, 100 and 200 bonds. The imposed bead number density is $\rho=0.85$. The filler particle radius $R$ was taken to be 2, 4, 8 and 12 in separate simulations. All dimensions are normalized by the unit cell size of the underlying lattice. Typically, the SAW procedure led to 200–400 chain overlaps, which are generally eliminated during the first 30,000 MC equilibration steps. The production phase was run for at least 5 million steps. The results were averaged over 20 replicas of the system. The replicas are statistically uncorrelated, each being a totally new realization of the system.

The flat wall case corresponds to the limit $R\rightarrow\infty$. In these simulations, the filler particle is eliminated and impenetrable flat wall conditions are imposed on two opposing surfaces of the simulation cell in Fig. 1. The periodic boundary conditions are preserved on the other faces of the cell. In this case, the coordinate $r$ is taken in the direction perpendicular to the two walls, and the size $L$ of the simulation cell is kept unchanged at 50. This confined film configuration leads to faster convergence of the averages because similar structure is generated in the vicinity of each wall and hence the number of replicas that need to be considered may be reduced by half.

The polymer structure next to the wall was monitored by dividing the polymer volume in bins in the radial direction, $r$, and by taking advantage of the spherical symmetry of the problem. The thickness of each bin was taken to be equal to one unit cell of the bcc lattice, except in the evaluation of the chain structure on the chain scale where the bin size is twice this value.

The number density was computed in each bin for both the overall bead population and for the chain end beads. The average bond orientation was evaluated based on the second Legendre polynomial $P_2^b=(1/2)(3\cos^2\theta_b-1)$, where the angle $\theta_b$ is made by the bond vector with the radial direction at the current site (Fig. 1). In the case of the flat wall, the radial direction is replaced by the normal to the wall. For random orientation of bonds, $P_2^b$ vanishes. A preferential orientation in the tangential direction leads to negative $P_2^b$ values. The direction tangential to a lattice sphere is defined here as being perpendicular to the line connecting the

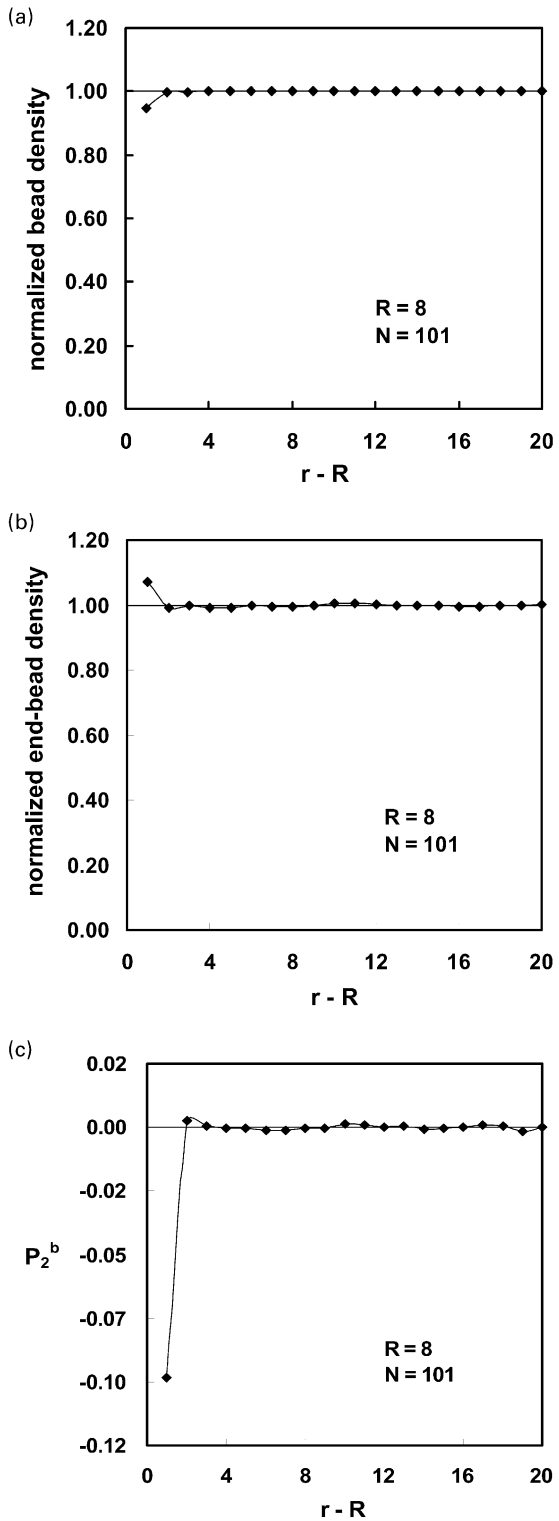


Fig. 2. The normalized bead number density (a), normalized chain end density (b) and the measure of bond orientation $P_2^b$ (c), as a function of distance from the wall, for the system with $R = 8$ and $N = 101$. The normalization is made with the respective bulk quantities. The uncertainty in computed values is largest at small $r - R$. Its maximum value here is 2%.

current bead with the center of the sphere. If all bonds are oriented in the tangential direction ($\theta_b = 90°$), $P_2^b = -0.5$. The orientation was also computed for chain segments of length $N_s = 4$ and 8, using a similar definition of the segment orientation, $P_2^s$. The angle $\theta_s$ is made by the end-to-end vector of the segment (between beads $i$ and $i + N_s$) and the radial vector passing through bead $i$. The segment is conventionally assigned to the bin in which bead $i$ resides. Results for a certain bin are obtained by averaging over all beads in that bin and over all replicas of the system.

## 3. Results and discussion

### 3.1. Polymer structure on the bond scale

The polymer structure was studied on the scale of a bond in the vicinity of curved (convex) and flat surfaces. Fig. 2 shows the results obtained for the system of $N - 1 = 100$ bonds per chain, and a filler particle of radius $R = 8$.

The bead number density variation with the distance from the surface of the particle ($r - R$) is shown in Fig. 2a. The plot is normalized by the bulk (nominal) density, $\rho$. The density at the wall is lower than that in the bulk (large $r - R$ in Fig. 2), situation similar to that encountered next to a flat wall. The wall limits the number of configurations a neighboring chain may take, which leads to an entropic force that drives the chains away from the interface. The depletion depends on the mean density, being more pronounced in low-density systems. When the (bulk) mean density increases, packing counteracts the effect of the entropic forces reducing depletion.

For completeness, we note that in simulations in which energetic effects are considered, the density at the wall depends on the relative importance of the energetic and entropic effects. For a flat interface and in the case in which the polymer chains interact with the wall through an attractive potential, the density is higher at the wall [17]. When there is no interaction with the wall, but the cohesive energy of the polymer is taken into account, the density is smaller at the wall compared to the bulk [18].

The normalized chain end density is shown in Fig. 2b. Enrichment in chain ends of about 10% is seen in the layer next to the wall, with a small opposite effect manifested in the next layer. The thickness of the polymer layer affected by the presence of the wall is essentially one bond length. The chain end segregation reported here is rather small compared with published data for the flat wall. As discussed below, the difference is due in part to the curvature of the wall. It is also known that lattice MC models predict less chain end segregation than similar off-lattice models.

Entropy driven chain end segregation to a flat impenetrable wall has been repeatedly reported in the literature [18, 29,30]. This effect is due to the fact that the number of forbidden chain configurations is larger for chains that do not end at the wall compared with those that have at least

one of the ends in the interface [6]. This provides an entropic driving force for chain end segregation.

Fig. 2c represents the measure of bond orientation, $P_2^b$. The bonds are preferentially oriented in the tangential direction (negative $P_2^b$) in the first layer next to the curved wall. A marginal opposite effect is seen in the second layer, which is correlated with the orientation in the first bin; for the bonds in the first layer to be oriented mostly parallel to the interface, it is geometrically necessary for the bonds in the adjacent layer to be preferentially oriented perpendicular to the interface. No preferential bond orientation is seen farther from the wall ($P_2^b = 0$). Similar effects have been observed for the flat interface in absence of energetic interactions; furthermore, an attractive interaction with the wall leads to adsorption and to a quasi-temperature-independent preferential orientation of bonds [16,17].

These results suggest that, when measured on the bond scale, the thickness of the 'perturbed polymer layer' is rather limited. In fact, energetic effects being absent, the thickness of this layer is given by the persistence length of the chain (chain stiffness). In the present case of essentially freely jointed beads, the persistence length is one bond only. Hence, the 'perturbed' polymer volume fraction being small, these observations do not support the 'bonded polymer layer' theory as a realistic description of the physics in this system.

Fig. 3 shows the variation of the chain end density and of $P_2^b$ with the chain length, both computed in the bin next to the wall. As expected, it is seen that an increase in chain length favors chain end segregation at the wall (Fig. 3a). The variation of $N$ has no effect on the bond orientation (Fig. 3b). In the athermal limit the preferential bond orientation is a purely geometric effect not influenced by the entropy, and hence independent of chain length. Although increasing the chain length leads to a larger entropic driving force for chain retraction from the wall, we see only a modest 2% reduction in the total density at the wall as the chain length changes from $N - 1 = 32–200$.

The effect of the particle curvature is also shown in Fig. 3. Results obtained for the flat wall are included for reference. The entropic force leading to chain end segregation is more important in the flat wall case. This is a consequence of the fact that the spherical excluded volume of the filler has a weaker effect in reducing the number of allowed chain configurations compared with the much more constraining flat wall. The data in Fig. 3 are re-plotted in Fig. 4 as a function of particle radius and for various chain lengths ($1/R = 0$ corresponds to the flat wall). No correlation is apparent between the two measures of the polymer structure discussed here, and the relative size of the filler and polymer chains (gyration radius). The dependence of the total density at the wall on wall curvature is not shown since this parameter is essentially insensitive to the wall curvature for the investigated range of $R$.

A weaker effect of wall curvature is observed on bond

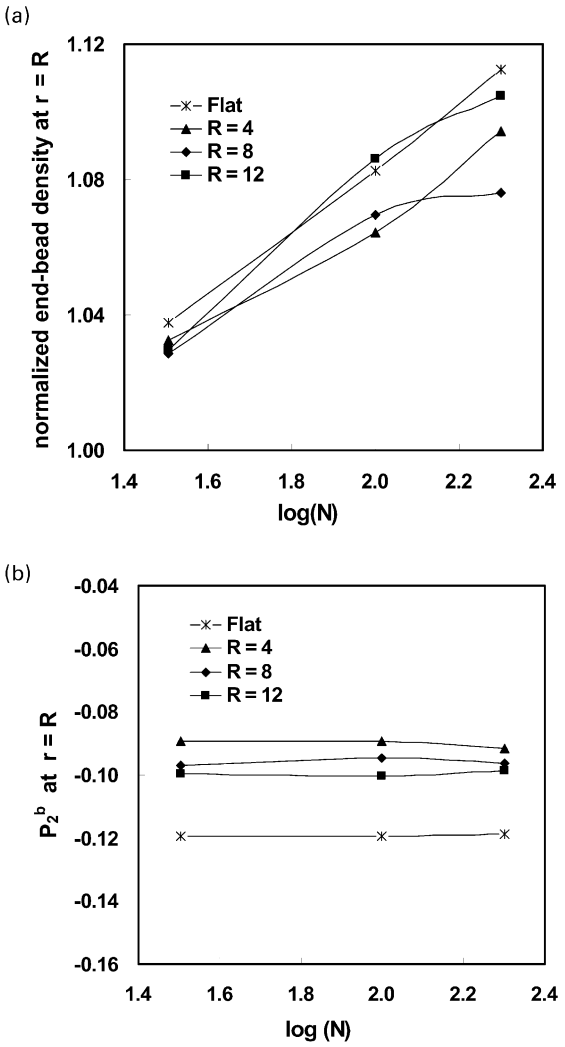


Fig. 3. Variation with the chain length of the normalized chain end number density (a) and of $P_2^b$ (b). The normalization is made with the respective bulk quantities.

alignment. The small fillers (large curvature) lead to less preferential orientation than the large particles and the flat surface. The thickness of the polymer layer in which bonds are preferentially oriented is independent of chain length and particle size.

Hence, when measured on the scale of a bond, the polymer structure does not appear to be significantly affected by the presence of the wall at distances larger than a bond length from the surface of the filler. Furthermore, increasing wall curvature leads to a further reduction of this effect. This is due to the absence of any persistence length along the chain. We conjecture that these conclusions remain valid in the athermal system when reducing the inter-filler spacing below a chain gyration radius since, on the scale of a bond, the presence of the wall is manifested only over one bond length within the polymer matrix. This conjecture needs to be verified by future simulations.

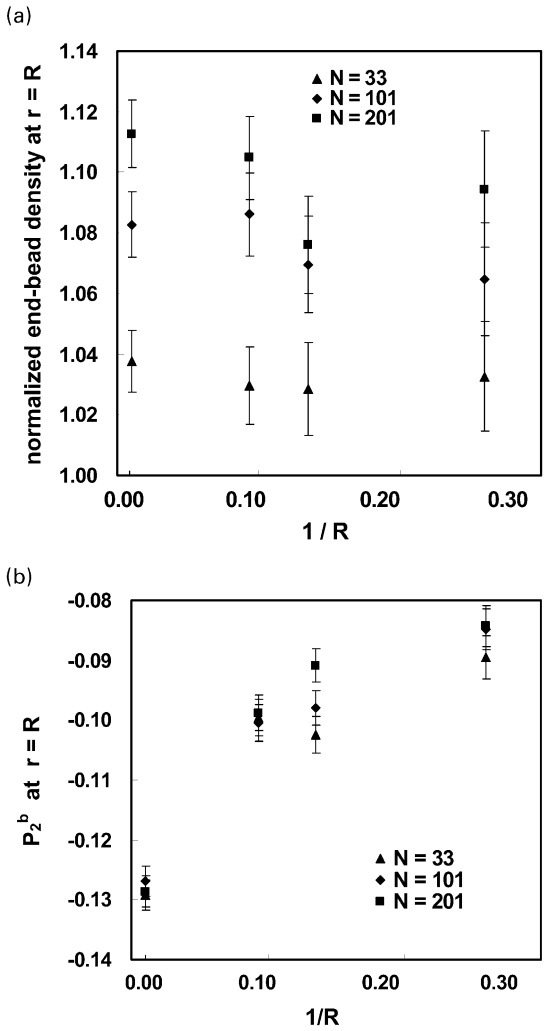


Fig. 4. Variation of the normalized chain end number density (a) and of $P_2^b$ (b) with the wall curvature. The normalization is made with the respective bulk quantities.

### 3.2. Polymer structure on the chain segment scale

The structure of the polymer probed on scales larger than the bond scale provides additional insight. To this end, $N_s = 4$ and 8 bond long chain segments are considered and the segment orientations as well as the end-to-end segment length are computed as a function of the distance from the surface of the particle. A segment connecting beads $i$ and $j$ belonging to the same chain is conventionally assigned to the bin in which bead $i$ resides. The system with $N - 1 = 100$ and $R = 8$ is considered in this analysis.

The end-to-end segment length is shown in Fig. 5 as a function of the distance from the surface of the filler, $r - R$. A chain segment ($N_s$ beads) in the bulk melt has an end-to-end distance of $R_{es}^2 = Cb^2(N_s - 1)$, where $C$ is a constant that accounts for the swelling of the chain with respect to the random walk due to its intrinsic stiffness (angles imposed by the lattice). In the present case of chains occupying a bcc lattice of unit cell size equal to one, the average bond length

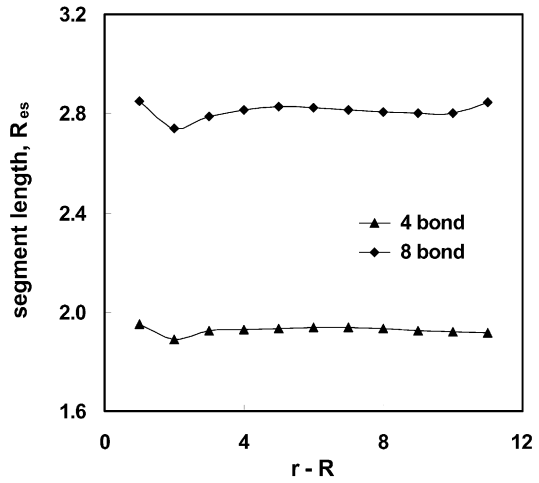


Fig. 5. End-to-end segment length as a function of the distance from the wall for segments of $N_s = 4$ and 8 bonds, and for the system with $R = 8$ and $N = 101$.

is $b = 0.92$. Based on the bulk segment lengths in Fig. 5 we obtain $C = 1.16$.

The segment length decreases by about 5% in the neighborhood of the particle. This contraction is the direct effect of the confinement on the SAW. However, the average length of the segments originating in the first bin is similar to that in the bulk. This is due to the fact that such vectors point into the bulk, away from the interface, and hence are not subjected to the (mainly radial) constraint imposed by the particle. The thickness of the layer in which the segment length is affected by the presence of the wall is on the order of the length of the segment considered (Fig. 5).

The variation of the average segment orientation $P_2^s$ with the distance from the wall is shown in Fig. 6 for the two segment lengths considered. The data in Fig. 2c, corresponding to the bond orientation are reproduced for reference. As with the bonds, the segments are preferentially oriented in the tangential direction. The thickness of the

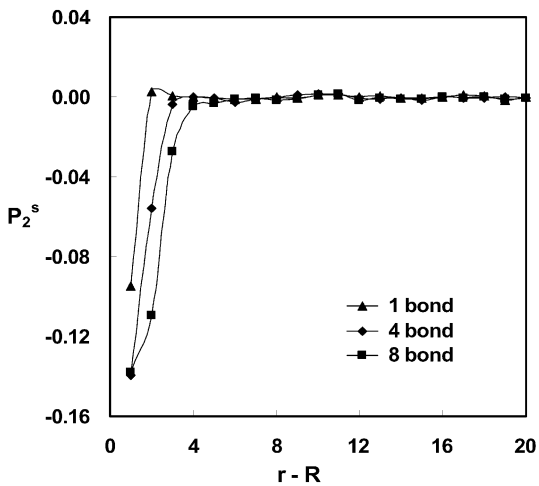


Fig. 6. Average segment orientation, $P_2^s$, as a function of the distance from the wall for segments of $N_s = 4$ and 8 bonds, and for the system with $R = 8$ and $N = 101$.

affected region is similar to that measured in Fig. 5, in connection with the variation of segment length. It correlates closely with the length of the probing segment, $R_{es}$.

The three curves may be obtained analytically based on a simple geometric argument according to which $P_2^s$ results by averaging the second Legendre polynomial over the surface of the sphere of radius equal to the length of the end-to-end vector, and centered at $r - R$ from the particle surface (Fig. 7). For averaging, all directions are allowed, except those that intersect the surface of the particle (dotted line in Fig. 7). This leads to the equation

$$P_2^s(x) = \frac{1}{4\pi}\int_0^{2\pi}\int_0^{\xi}\frac{1}{2}(3\cos^2\theta - 1)\sin\theta\,\mathrm{d}\theta\,\mathrm{d}\varphi. \quad (1)$$

The two parameters $x$ and $\xi$ are defined in Fig. 7. In the figure, $S$ represents the length of the end-to-end vector considered.

The data in Figs. 5 and 6 and those in Figs. 2 and 3 suggest that, in the athermal limit, the volume of polymer affected by the presence of the solid wall depends on the probing metric. The thickness of this region is independent of chain length as long as the chains are longer than the probing segment. Published results support this observation. Wattenbarger et al. [31,32] studied chain conformations next to a flat wall in the athermal limit in both 2D and 3D and determined that the effect of the surface on the average chain dimensions (sampling on the chain scale) extends about twice the radius of gyration within the polymer matrix, or approximately one end-to-end distance [12]. Baschnagel and Binder [17] identify several length scales characterizing the size of the interfacial region. In their non-athermal system, these parameters vary with temperature. When the cohesive energy in the polymer is taken into account, the thickness of the interfacial layer measured on the scale of the chain becomes dependent on the value of the cohesion energy, with the thickness decreasing with increasing cohesion [18]. However, when correcting for the effect of the cohesion energy on the chain end-to-end vector, the thickness results to be approximately one end-to-end distance as found in the present case.

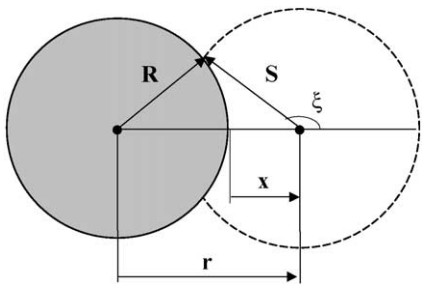


Fig. 7. Schematics of allowable directions for the segment end-to-end vector in the vicinity of a curved wall (radius of curvature $R$). $S$ represents the bulk length of the end-to-end vector considered. Segments that intersect the surface of the particle are not allowable due to the excluded volume constraint. $P_2^s$ may be obtained by averaging over the sphere of radius $S$ shown by the dotted line.

This observation is relevant for the interpretation of experimental results. In experiments, the structure of the polymer matrix is probed with a radiation of certain wavelength and only features on that length scale are detected. The present analysis suggests that the measured thickness of the 'bonded polymer layer' about each particle should be on the order of the probing wavelength. Hence, the volume of perturbed polymer evaluated from such measurement depends on the wavelength of the probing radiation and the total interfacial area in the material.

### 3.3. Polymer structure on the chain scale

The structure on the chain scale is studied next. A good measure of the chain size and shape is the gyration tensor $G_{ij}$ [33]. For a chain of $N$ beads, the tensor reads

$$G_{ij} = \frac{1}{N}\sum_{k=1}^{N}\left(X_i^k - X_i^{\mathrm{CM}}\right)\left(X_j^k - X_j^{\mathrm{CM}}\right) \quad (2)$$

where $\mathbf{X}^k = \{X_1^k, X_2^k, X_3^k\}$ is the position vector of bead $k$, and CM stands for the center of mass of the current chain. The trace of this tensor equals the mean square radius of gyration of the chain, $R_g^2$.

The chains are not spherical in the bulk, with their large semi-axis being $\sqrt{\langle\lambda_1\rangle}$, where $\langle\lambda_1\rangle$ is the system average the largest eigenvalue of $\mathbf{G}$. Fig. 8a shows the three eigenvalues for chains having their center of mass at various distances from the center of the filler. In the bulk, at large $r - R$, the three eigenvalues are $\langle\lambda_1\rangle = 15.2$, $\langle\lambda_2\rangle = 3.4$, $\langle\lambda_3\rangle = 1.3$, which suggests that the chain is a flattened ellipsoid. The ratio of the three eigenvalues is 11.7:2.6:1, while the corresponding ratio obtained from a random walk is 12.07:2.72:1 [34]. The three average eigenvalues sum up to 19.9, which equals the mean square radius of gyration computed by

$$\left\langle R_g^2\right\rangle = \frac{1}{N}\left\langle\sum_{k=1}^{N}(R^k - R^{\mathrm{CM}})^2\right\rangle,$$

as it should. Here, $R^{k,\mathrm{CM}}$ are position vectors of bead $k$ and of the center of mass, respectively. The large semi-axis (the eigenvector corresponding to the largest eigenvalue) is randomly oriented in space. This provides another measure of the isotropy of the bulk after equilibration.

Chains that are close to the filler are distorted (Fig. 8a). Interestingly, the distortion is more pronounced in the direction of the large semi-axis and for chains having their center of mass within the filler, i.e. those that 'wrap around' the spherical particle. The chains having their center of mass in the first bin (here of thickness 2) next to the filler surface are essentially undistorted. This may occur only if the ellipsoids rotate next to the filler with their large semi-axis in the direction tangential to the sphere. A similar observation was made for the flat interface and in absence

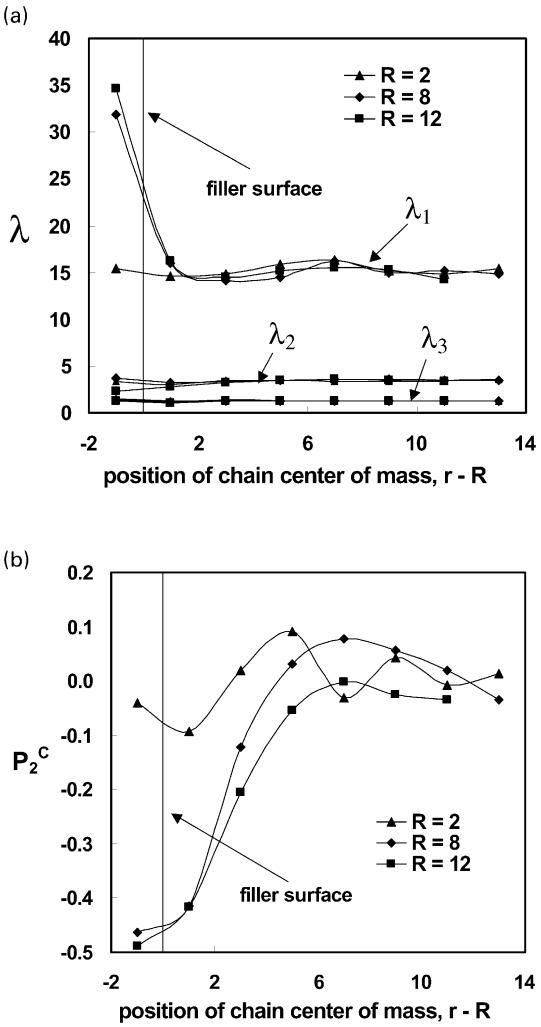


Fig. 8. (a) Variation of the eigenvalues of the gyration tensor **G** with the distance between the chain center of mass and the wall. The chains are flattened ellipsoids in the bulk, with $\lambda_1 > \lambda_2 > \lambda_3$. Chains with the center of mass within the filler are elongated in the direction of the large semi-axis of the ellipsoidal coil. Each data point corresponds to a radial bin of thickness 2. The largest error bar on measured quantities (for smallest $r - R$) is 4%. (b) Variation of $P_2^c$ with the distance between the chain center of mass and the wall. Chains with their center of mass closer than a rms radius of gyration from the filler surface tend to orient with their large semi-axis in the direction tangential to the spherical filler ('docking' transition). The error bar on measured quantities is no larger than $\pm 0.1$.

of strong attractive interaction between polymer and wall [15]. As observed here, chains do not undergo an adsorption transition, but rather they are 'docking' to the filler particle.

Furthermore, the results obtained for filler radii $R = 8$ and 12 are similar. In both cases, the filler radius is larger than the radius of gyration of the chains. When this relationship reverses (e.g. for $R = 2$), the filler may be placed within a chain coil without significantly distorting it.

These conclusions are supported by the data shown in Fig. 8b which represents the variation of $P_2^c$ with the position of the chain center of mass with respect to the center of the spherical filler. $P_2^c$ is the second Legendre polynomial computed based on the angle made by the line connecting the filler center and the chain center of mass, and the eigenvector corresponding to the largest eigenvalue of the gyration tensor **G**. Negative $P_2^c$ values represent preferential orientation of the ellipsoidal chains with their large semi-axis in the direction tangential to the spherical filler. The chains having their center of mass within the filler are fully aligned, as expected ($P_2^c = -0.5$). Chains having their center of mass as far as one rms gyration radius away from the wall are preferentially aligned. Again, the degree of alignment is independent of filler radius once this is larger than the rms radius of gyration of the chains. No preferential alignment is seen in the case of the smallest filler ($R = 2$).

### 3.4. Chain mobility

The chain mobility was evaluated as a function of the distance from the solid wall. The mean square displacement of beads is used as a measure of mobility. The diffusion coefficient may be derived from this quantity in the long time limit.

Simulating chain dynamics in MC models is not as straightforward as in models that incorporate real time (e.g. molecular dynamics). In general, it must be insured that only moves that perturb the structure locally are allowed. With this precaution, it has been reported in the literature that one recovers in MC simulations the Rouse dynamics, the cross-over to reptation and the free diffusion of the chain [28].

As in the previous analysis, the polymer volume about the filler is divided in spherical bins, each bin having a thickness of 2. The beads are assigned to the bin in which they reside at time zero. The trajectory of each bead is traced for a relatively short period of time (~3000 MCS) during the production phase, and the mean square displacement in the radial and tangential directions is computed. These quantities are averaged over all beads in the respective bin and over all replicas of the system. The trajectory is traced for a short time interval such that the beads do not travel excessively, which would render artificial their assignment to the bin from which they originate.

The results obtained in this study are similar to those for the flat interface. The bead diffusion coefficient in the direction tangential to the wall is similar to that in the bulk, even though the bead density at the wall is lower than the bulk value. This is due to the fact that the depleted layer is rather thin (one bond length only) and even the chains that wrap around the filler have most of their beads in the region with bulk density. Therefore, their mobility must be that of the bulk. The mobility in the direction normal to the wall is reduced for beads located in the first bin (within a distance of 2 from the wall) and is similar to the bulk value at larger distances. The chain mobility was not evaluated, but it is expected that those chains having beads in the first bin have a lower mobility in the radial direction than those in the bulk.

## 4. Conclusions

The polymer structure and mobility in the vicinity of a curved impenetrable interface was studied by means of lattice Monte Carlo simulations in the athermal limit using the bead-spring model. It was observed that the bead number density is lower at the wall than in the bulk and that the chain ends segregate at the wall. These effects increase with increasing chain length. The wall induces preferential bond and chain segment orientation in the tangential direction. The thickness of the perturbed polymer layer depends on the probing metric. This suggests that experimental measurements of the perturbed polymer volume in a nanocomposite or a polymeric thin film depend on the radiation wavelength used for probing. The degree of preferential orientation does not depend on chain length and decreases with increasing wall curvature. The chains have the shape of a flattened ellipsoid in the bulk. Next to the wall, they rotate with their large semi-axis in the direction tangential to the spherical wall, with no change of coil size ('docking' transition). Fillers having radii larger than the rms gyration radius of the chain lead to similar structure on the scale of the chain, while smaller fillers leave both the size and the orientation of the coils unperturbed. The bead mobility in the direction tangential to the wall is similar to that in the bulk. Normal to the spherical filler, the bead mobility is smaller in the immediate neighborhood of the wall and recovers the bulk value at larger distances.

## Acknowledgments

This work was supported by the National Science Foundation through grant CMS 9908025 and by the Office of Naval Research through grant N00014-01-1-0732. The authors thank to an anonymous reviewer for valuable comments.

## References

[1] Stamm M. Adv Polym Sci 1992;100:357.
[2] Factor BJ, Russel TP, Toney MF. Macromolecules 1993;26:2847.
[3] Forrest JA, Dalkoni-Veress K, Stevens JR, Dutcher JR. Phys Rev Lett 1996;77:2002.
[4] Sen S, Cohen JM, McCoy JD, Curro JG. J Chem Phys 1994;101:9010.
[5] Theodorou DN. Macromolecules 1988;21:1391.
[6] de Gennes PG. Adv Colloid Interf Sci 1987;27:189.
[7] Scheutjens JMHM, Fleer GJ. J Phys Chem 1979;83:1619.
[8] Scheutjens JMHM, Fleer GJ. Macromolecules 1985;18:1882.
[9] Zhan Y, Mattice WL. Macromolecules 1994;27:7056.
[10] Mansfield KF, Theodorou DN. Macromolecules 1991;24:6283.
[11] Kumar SK, Vacatello M, Yoon DY. Macromolecules 1990;23:2189.
[12] Yethiraj A. J Chem Phys 1994;101:2489.
[13] Eisenriegler E, Kremer K, Binder K. J Chem Phys 1982;77:6296.
[14] Bitanis IA, ten Brinke G. J Chem Phys 1993;99:3100.
[15] Bellemans A, Orban J. J Chem Phys 1981;75:2454.
[16] Jang JH, Mattice WL. Polymer 1999;40:4685.
[17] Baschnagel J, Binder K. Macromolecules 1995;28:6808.
[18] Cifra P, Nies E, Karasz FE. Macromolecules 1994;27:1166.
[19] Chhajer M, Gujrati PD. J Chem Phys 1997;106:8101.
[20] Petrovic ZS, Javni I, Waddon A. Proc ANTEC 1998;2390.
[21] Ng C, Schadler LS, Siegel RW. J Nanostruct Mater 1999;12:507.
[22] Vollenberg PHT, Heikens D. Polymer 1989;30:1656.
[23] Vollenberg PHT, deHaan JW, van de Ven LJM, Heikens D. Polymer 1989;30:1663.
[24] Zhu AJ, Sternstein SS. Mater Res Soc Proc 2001;661.
[25] Reichert WF, Goritz D, Duschl EJ. Polymer 1993;34:1216.
[26] McCrackin FL. J Chem Phys 1967;47:1980.
[27] Landau DP, Binder K. Monte Carlo simulations in statistical physics. Cambridge: Cambridge University Press; 2000.
[28] Keer T, Baschnagel J, Muller M, Binder K. Macromolecules 2001;34:1105.
[29] Kajiyama T, Tanaka K, Takahara A. Macromolecules 1997;30:280.
[30] Pakula T. J Chem Phys 1991;95:4685.
[31] Wattenbarger MR, Chan HS, Evans DF, Bloomfield VA, Dill KA. J Chem Phys 1990;93:8343.
[32] Chan HS, Wattenbarger MR, Evans DF, Bloomfield VA, Dill KA. J Chem Phys 1991;94:8542.
[33] Cannon JW, Aronovitz JA, Goldbart P. J Phys I 1991;1:629.
[34] Janszen HWHM, Tervoort PA, Cifra P. Macromolecules 1996;29:5678.